Microscale Contact Formation by Laser Enhanced Contact Optimization

Stephan Großer, Eve Krassowski, Sina Swatek, Hongming Zhao, and Christian Hagendorf

***Abstract*—A technique to improve contacts of solar cells laser enhanced contact optimization (LECO) has been studied in terms of micro scale contact formation at industrial PERC solar cells. High-resolution diagnostics by focused ion beam techniques and scanning electron and transmission electron microscopy indicate the LECO-induced formation of microscopic contacts at the buried interface between the screen-printed silver finger and the silicon wafer. A large quantity of these micro contacts where found exclusively for LECO processed cells. Target preparation and three-dimension cross-section investigation reveal an interdiffusion of the Ag and Si material as the underlying root cause for improved local contact resistivity. We propose a descriptive model for local ohmic contact formation maintaining surface passivation.**

***Index Terms*—Contact formation, microstructure analysis, solar cell.**

I. Introduction

METAL semiconductor contacts are commonly made by screen printing of metal pastes on the Si wafer and the formation of low-ohmic contacts has been a major topic in research over the years [1]–[3]. A process for contact improvements is laser-enhanced contact-optimization (LECO), which has been reported previously [4], [5]. Contrary to other used laser-based treatments within the cell manufacturing process, like laser cutting [6], laser edge isolation [7], laser fired contacts [8], and laser doped selective emitters [9], in the LECO treatment, the laser is used for nondestructive carrier injection, whereas the driving force of the treatment is the current induced by the LECO process. The process takes place after the fast firing process of screen-printed solar cells. After the LECO treatment solar cells show a strongly reduced contact resistance allowing the contact formation even on low-doped emitters [5]. New pastes adapted for the LECO process have been reported [4], [10] exhibiting also improved open-circuit voltages as well as a small increase in short-circuit current.

We present in this contribution a first microstructure analysis of the contact formation at the silver grid finger and the silicon wafer interface. Based on focused ion beam (FIB) target preparation and scanning electron microscopy (SEM) defect diagnostics the local material properties of the interface are studied before and after LECO treatment. Based on extended cross-section investigations we identify microscopic structural modifications that are assumed to be related to the LECO treatment as a potential root cause for the contact enhancement. A first proposal for a physical model of LECO contact formation will be discussed.

II. Experimental

To study the impact of the LECO treatment on the contact formation industrial off-spec 5 busbar p-type passivated emitter and rear cell (PERC) solar cells with very high contact-resistance were used. For comparison of the microstructure of the formed contact interface (before and after LECO treatment) it is crucial that the initial contact microstructure is identical. Hence, a single solar cell meets the demands in terms of the equal material (wafer, paste) and cell process conditions. Therefore, single solar cells with a homogeneously high contact resistance were selected judging by electro luminescence (EL) imaging. Then, one half of a solar cell was kept untreated while the other half of the solar cell was treated with the LECO process. The LECO treatment was performed on the commercially available LECO Labtool by CE Cell Engineering with a processing time of 0.8 s (half-cell). As described in [5] during the LECO process a focused laser beam laterally scans the cell, inducing charge carriers locally. Free carriers are separated by applying a reverse bias, resulting in a high reverse current.

After the LECO processing the pieces of the solar cell were separated by mechanical scribe and cleavage for detailed contact structure analysis. Cross sections and transmission electron microscopy (TEM)-lamellae of contacts have been made by FIB preparation and imaging by SEM using ZEISS Auriga 40 (Carl Zeiss Microscopy GmbH) and FEI Versa 3D (Thermo Fisher Scientific Inc.) cross-beam systems. To expose contact interfaces underneath the silver paste, selective removal of silver and/or glass have been performed with standard HF and HNO_3-etching methods. Before and after selective etching microstructure investigations have been performed by SEM using an analytical

Manuscript received June 15, 2021; revised September 2, 2021 and November 15, 2021; accepted November 16, 2021. Date of publication December 6, 2021; date of current version December 23, 2021. This work was supported by the Federal State Saxony-Anhalt through EFRE Founding within the project ERNST under Contract 1904/00005. *(Corresponding author: Stephan Großer.)*

Stephan Großer, Sina Swatek, and Christian Hagendorf are with the Fraunhofer Center for Silicon Photovoltaics CSP, 06120 Halle (Saale), Germany (e-mail: stephan.grosser@csp.fraunhofer.de; sina.swatek@csp.fraunhofer.de; christian.hagendorf@csp.fraunhofer.de).

Eve Krassowski is with the Fraunhofer Center for Silicon Photovoltaics CSP, 06120 Halle (Saale), Germany, and also with CE Cell Engineering GmbH, Orionstraße 1, Industriegebiet Star Park, 06184 Kabelsketal, Germany (e-mail: e.krassowski@cell-engineering.de).

Hongming Zhao is with CE Cell Engineering GmbH, Orionstraße 1, Industriegebiet Star Park, 06184 Kabelsketal, Germany (e-mail: h.zhao@cell-engineering.de).

Color versions of one or more figures in this article are available at https://doi.org/10.1109/JPHOTOV.2021.3129362.

Digital Object Identifier 10.1109/JPHOTOV.2021.3129362

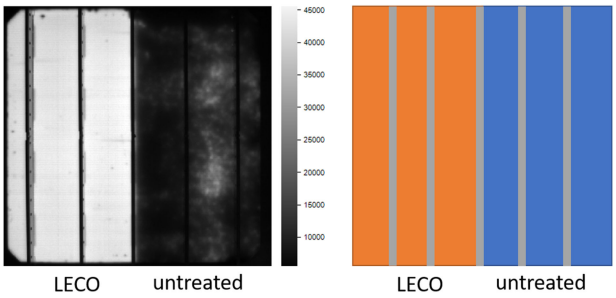

Fig. 1. EL image (left) of a solar cell with former homogeneous high contact-resistance after half-side LECO treatment (scheme on the right).

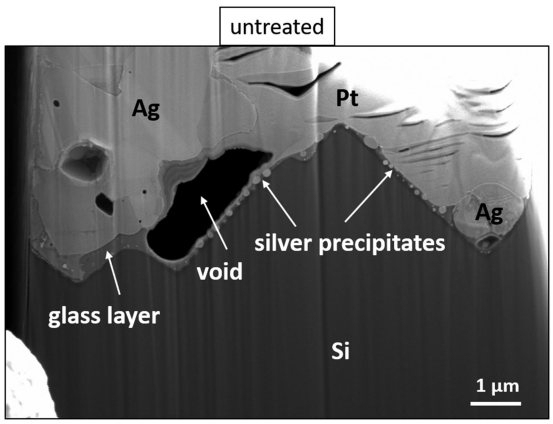

Fig. 2. SEM image of a FIB prepared cross section of an untreated contact for inspection of the interface between silver metallization and silicon.

FE-SEM SU-70 (Hitachi Inc.) instrument. From a LECO treated contact (without any selective etching of the silver paste) an electron transparent lamella of the contact interface has been prepared out by the *in situ* lift-out technique [11] and low voltage polishing by FIB. The microstructure of the contact interface was investigated using high-resolution transmission electron microscopy, and energy-dispersive X-ray (EDX) spectroscopy. For this purpose, a TEM/STEM from FEI Titan^{3}G2 60–300 equipped with a Super-X Si-drift EDX-detector system (FEI Thermo Fisher Scientific Inc.) and GIF Quantum (Gatan imaging filter; Gatan Inc.) was utilized.

III. Results

Fig. 1 shows the EL image and application scheme after LECO treatment with clear improvement of the contact resistance of the left half-side visible by a homogeneous EL. After the LECO treatment parts of the LECO treated and parts of the untreated cell area were prepared for microstructure analysis of the contact.

The solar cell has been prepared for high-resolution microstructure analysis at the contact formed between silver finger and silicon wafer. After FIB cross-section preparation, a representative SEM image of the LECO untreated contact interface structure is shown in Fig. 2. The found contact-interface structure exhibits the silver metal of the grid finger, a glass layer with incorporated Ag-precipitates and the silicon wafer. A

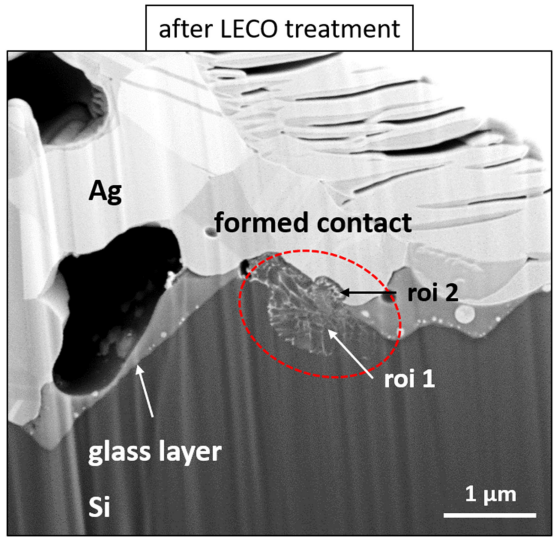

Fig. 3. SEM image of a FIB prepared cross section of the LECO treated contact.

Pt-protection layer results from the FIB-preparation and protects the surface from damage. No distinctive features in the contact structure were found on multiple observed cross sections. The observed structure is consistent with the literature [1], [3], [12]–[15].

Modifications of the contact after LECO processing have been investigated at the LECO treated part of the cell. Multiple FIB cross sections have been prepared using the sequential slice and view technique at different finger positions to expose the contact interface after treatment. Fig. 3 shows a SEM image of the contact interface and exhibits in large parts a contact structure comparable to the initial state. Noticeable is a unique contact-structure modification at the contact interface (highlighted in Fig. 3), which was found solely after LECO treatment. This feature occurs locally and distributed at the contact interface and has been found often at different LECO treated contact positions. All found formed contacts were near or on top of the pyramid peaks. An estimation of the LECO-formed contact density (contacts per area) indicates a value of roughly $5{\cdot}10^6$ cm^{-2} for the investigated solar cell contact.

Fig. 3 exhibits also a first insight in the microstructure of the contact interface modification with two distinct regions of interest (roi). Within the silicon a filament shaped bright material contrast was found (roi 1) indicating the occurrence of an additional element in the silicon with higher atomic number. Within the range of the formed contact silver must be incorporated into the silicon. Adjacent, a noticeable area has been formed within the Ag-finger (roi 2), which appears darker than the surrounding Ag. Most probably the structure arises from the incorporation of silicon into silver and vice versa forming a composition of different fractions. It is known in silicon technology that a silicide can form ohmic contacts [16]. To proof our assumption of Ag/Si interdiffusion an analysis with higher spatial resolution was needed to prevent artifacts. An electron-beam transparent lamella of a buried LECO formed contact has been prepared out of the solar cell contact finger by FIB-technique. TEM has

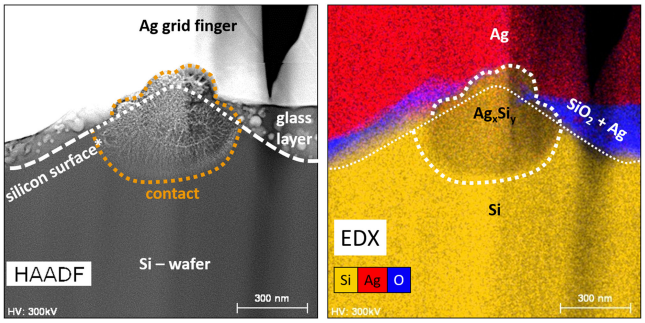

Fig. 4. Left: HAADF-STEM image of a formed contact after LECO treatment with dashed lines as indications "white" for the supposed initial silicon surface (*) before LECO treatement) and "orange" for the modified area. Right: Corresponding element distribution map obtained by EDX technique.

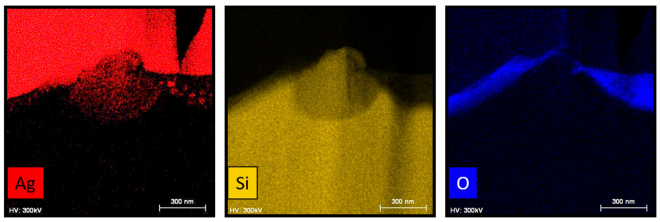

Fig. 5. Separated maps of the integrated intensities of element-characteristic X-ray signals from the EDX image overlay (see Fig. 4) of Ag, Si, and O with enhanced contrast.

been conducted and revealed the composition of the formed contact cross section. Fig. 4(left) shows the HAADF-STEM (High angle annular dark-field scanning transmission electron microscopy) image of the contact interface below the Ag-grid finger to the emitter surface of the wafer. As a guide to the eye a white dashed line is drawn indicating the former supposed silicon surface (before treatment) and an orange line for the modified contact area. The indication of the supposed former silicon surface is based on the visible silicon surface outside and the extrapolation of the surface line inside the formed contact. One can observe a microstructure change at the supposed former interface with a dimension of $\sim$ 600 nm in width and $\sim$ 400 nm in height. Bright fiber-like structure above (in silver paste) and below (in silicon wafer), with more delicate fibers than in the silver paste, is visible. One has to keep in mind that the size does not necessarily match with the depth of the formed contact because the TEM image shows a random cross section due to the fact that the lamella was not cut out perpendicular to the pyramid surface normal direction. A corresponding element distribution was measured by means of EDX spectroscopy and is shown on the right-hand side of Fig. 4 as an overlay of Ag, Si, and O, the matrix elements. Element-specific EDX-maps, used for the overlay in Fig. 4, are shown separately in Fig. 5 to present the Ag distribution distinctly and visible. The composition of the formed contact structure was found as a fraction of Si and Ag in variable parts. By approximation based on the EDX data a silver fraction below 20 at. % was determined in the silicon substrate (roi 1). Hence, it could be verified that LECO induces an interdiffusion of silicon and silver, forming local sub-μm size point-contacts.

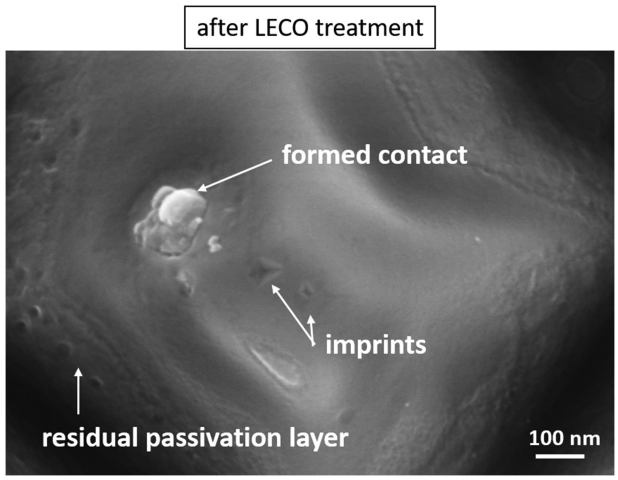

Fig. 6. Top-view SEM image of the contact interface after the removal of the grid finger (silver and glass) by a selective chemical etch. The pyramid peak is near the image center.

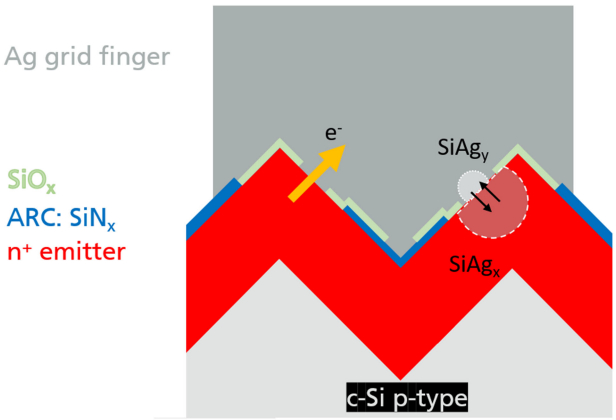

Fig. 7. Proposed model of the CFC formation due to LECO treatment.

Since cross-sections investigate a buried structure on local position the areal interface of the contact has been studied by top view imaging as well to proof the LECO formed contacts. Formed hill-like structures should be found on top of the silicon surface. The LECO treated solar cell has been prepared by chemical etching to remove the grid finger (silver, the glass, and the silver crystallites) and expose the wafer surface. Fig. 6 shows a SEM image in top view of a representative position of the contact interface with a single pyramid peak in the middle of the image. Imprints formed by Ag crystallites and residual SiN_x passivation layer can be seen which was found comparable to the initial contact structure. LECO formed contacts like found in the cross sections have been found on the pyramid surfaces as well.

Based on the obtained microstructure results of the current-fired contacts (CFC) we propose a first schematic model of the contact structure and the presumed contact formation phases during LECO treatment (Fig. 7).

In the first phase a local current is induced by a local laser beam in combination with the applied bias voltage on the solar

cells front side. In detail, the laser beam induces charge carriers in the depletion zone and causes a very local current flow at reverse bias conditions. Preferential paths of the current are the local low-resistive paths which must already exist between emitter and Ag metallization underneath the grid finger region. Highly resistive interface areas will not contribute to the current flow, whereas local low-resistance contact points at the semiconductor metal interface form at microscopic scale during the firing process [12]. The lowest resistance is expected at a position where Ag is contacting the silicon emitter with negligible glass interface layer. Low-resistance contact-points represent only a small fraction of the total contact interface area. Therefore, the total current will flow along a small area fraction with low-resistive current paths and results in high current-densities. These paths can be found on top or near the peak of the pyramids due to the absence of insulating residual passivation layer.

In the second phase of the contact formation, high current-densities lead to considerable power loss resulting in hot spots at the interface. As a result of the local generated heat a current-induced firing takes place at this particular point and Ag and Si diffuse into each other. Based on our observation of the solidified contact shape an isotropic element propagation originating from an interfacial contact point is presumable.

The third phase occurs during cooling down of the fired contact points. While laser scanning of the cell surface, local optical excitation of charge-carriers will be induced in a time interval defined by the laser excitation duration. Subsequent, current-induced thermal heating will extend into the range of μs to ms which is typically limited by local mean charge carrier lifetime. Since in the proximity of the molten contact the temperature is assumed to be considerably lower, the temperature will rapidly decrease due to the enhanced heat-dissipation into surrounding silver and silicon material.

The proposed schematic model allows a rough estimation of the expected current densities, needed to form current fired contacts at the interface between Ag and doped-Si. By consideration of the following assumptions, a local excitation and neglecting the time-dependence a simplified expression for the expected current density J_{LECO} during CFC formation can be given by

$$J_{\mathrm{LECO}} = \frac{I_{\mathrm{LECO}}}{A} \approx \frac{I_{\mathrm{LECO}}}{w \cdot l \cdot (A_{\mathrm{CFC}} \cdot D_{\mathrm{CFC}})}. \quad (1)$$

For simplification in (1), the current induced by the LECO process is assumed to flow exclusively through the low-resistance contact points in which the remaining grid finger/emitter interface is expected to be nonconducting. This is reasonable for solar cells with high contact resistivities. Estimated characteristic values of the measured current induced by LECO ($I_{\mathrm{LECO}} = 1$ A), the finger width ($w = 40$ μm), the affected finger length ($l = 1000$ μm), the found LECO-formed contact density (contacts per area $D_{\mathrm{CFC}} = 5{\cdot}10^4$ mm^{-2}) and the observed CFC interface area ($A_{\mathrm{CFC}} = 0.008$ μm²) result in a current density estimation of $J_{\mathrm{LECO}} \approx 64$ kA mm^{-2}. Tilke *et al.* [17] investigated current density limits in high-phosphorous doped-Si nanowires where the maximum current density before melting was found to be around 40 kA mm^{-2}. The comparison with reported melting limits at extreme large current densities indicate that the estimation in (1) based on our model is plausible at least in terms of the magnitude.

For a more detailed understanding and number of material properties and energy dissipation time constants are needed. However, the interdiffusion of silver and silicon is limited by the cooling down of the material system. The eutectic reaction of the Ag–Si system is around 848 °C and 89 at.% Ag with a negligible solubility of Si in Ag in the solid phase, as reported in [18]. We believe that the observed fiber-like Ag structure, visible in Fig. 4, results from the segregation of excess Ag in the Ag_xSi_y phase during a fast cooling step. A local and a low-ohmic metal-semiconductor contact is formed.

Nevertheless, for solar cells the electrical conductivity at the metal-semiconductor interface of silver front side metallization pastes sintered on silicon solar cells is dominated by other mechanisms [1]–[3], [12]–[14]. In this case, the current transport is based on electron tunneling through the glass layer due to Ag precipitates and dissolved Ag in the glass as well as Ag crystallites grown in the silicon surface. We also observed the presence of these structures in the investigated contacts before as well as after LECO treatment but did not find clear evidence, by direct comparison, that LECO impacts Ag precipitate or interface crystallite structures so far. Furthermore, current-injection firing of Ag-paste in a boron emitter is reported to generate additional silver dendrites in the glass layer [19]. Therefore, our model proposes the CFC as an additional current path within the total current transport. As a consequence of that model, for standard solar cells with already low contact resistivities the share of the current transport through CFCs will be low compared to the already existing paths due to less or smaller CFC generation.

IV. Conclusion

LECO has been applied to an industrial PERC solar cell and reduced the contact resistance by forming low-ohmic contacts. In the experiment one-half side of the full cell was LECO treated to guarantee a comparability of initial and LECO treated contacts. Structure investigations show no modification on the metal or cell like melting/sintering of the Ag-finger but changes were identified at the metal-finger semiconductor interface. A comparison of the contact interface reveals the LECO induced formation of an Ag_x and Si_y containing phase contacting the silver paste and the silicon (emitter). Silver was diffused into the silicon wafer (emitter) and silicon into the silver paste. We proposed a first model for the CFC formation by LECO treatment which explains the results found by microstructural analysis. Inhomogeneities in the contact resistance at the interface, more precisely low-ohmic current paths, lead to hot spots during the LECO process, Ag and Si interdiffusion and formation of low-ohmic metal semiconductor contacts after a rapid cooling. Finally, the buried contact-interface underneath the silver grid finger consists of a surface density around 0.05 μm^{-2} of

low-ohmic contact points (CFCs). Since CFCs are generated punctual the unaffected interface between finger and wafer would be preserved, reducing the fraction of recombination active metal-semiconductor interfaces.

A more detailed understanding of the CFC formation process is needed to further optimize the efficiency gain by LECO. Nevertheless, this basic model gives a first inside in the punctual contact formation mechanism, allows an understanding of the LECO working principle and enables future detailed characterization of the formed CFCs. Extensions of the model are supposed to improve LECO applications like selective contacting of low-doped emitters or optimization of metal pastes.

Acknowledgment

The authors would like to thank D. Ulm for sample preparation and SEM measurements as well as A. Hähnel for the TEM analysis.

References

[1] G. Schubert, F. Huster, and P. Fath, "Physical understanding of printed thick-film front contacts of crystalline Si solar cells—Review of existing models and recent developments," *Sol. Energy Mater. Sol. Cells*, vol. 90, pp. 3399–3406, 2006.

[2] J. Qin, W. Zhang, S. Bau, and Z. Liu, "Study on the sintering and contact formation process of silver frontside metallization pastes for crystalline silicon solar cells," *Appl. Surf. Sci.*, vol. 376, pp. 52–61, 2016.

[3] P. Kumar, M. Pfeffer, B. Willsch, and O. Eibl, "Contact formation of front side metallization in p-type, single crystalline Si solar cells: Microstructure, temperature dependent series resistance and percolation model," *Sol. Energy Mater. Sol. Cells*, vol. 145, pp. 358–367, 2016.

[4] R. Mayberry, K. Myers, V. Chandrasekaran, A. Henning, H. Zhao, and E. Hofmüller, "Laser enhanced contact optimization (LECO) and LECO-Specific pastes – A novel technology for improved cell efficiency," in *Proc. 36th Eur. Photovolt. Sol. Energy Conf. Exhib.*, 2019.

[5] E. Krassowski, S. Großer, M. Turek, and H. Höffler, "Laser enhanced contact optimization – a novel technology for metal-semiconductor-contact optimization for crystalline silicon solar cells," in *Proc. 37th Eur. Photovolt. Sol. Energy Conf. Exhib.*, 2020.

[6] J. Röth, N. Bernhard, C. Belgardt, M. Grimm, and F. Kaule, "Thermal laser separation (TLS) dicing process study – A new technology for cutting silicon solar cells for high-efficiency half-cell modules," in *Proc. 31st Eur. Photovolt. Sol. Energy Conf. Exhib.*, 2017, pp. 716–718, doi: 10.4229/EU-PVSEC20152015-2AV.3.2.

[7] O. Haupt, A. Schoonderbeek, L. Richter, R. Kling, and A. Ostendorf, "A new process for laser edge isolation of crystalline solar cells," in *Proc. 23rd Eur. Photovolt. Sol. Energy Conf. Exhib.*, 2008, pp. 1374–1376, doi: 10.4229/23rdEUPVSEC2008-2CV.4.15.

[8] E. Schneiderlöchner, R. Preu, R. Lüdemann, and S. Glunz, "Laser-Fired rear contacts for crystalline silicon solar cells," *Prog. Photovolt. Res. Appl.*, vol. 10, pp. 29–34, 2002, doi: 10.1002/pip.422.

[9] U. Jäger, A. Wolf, B. Steinhauser, J. Benick, J. Nekarda, and R. Preu, "Laser doping for high-efficiency silicon solar cells," *Proc. SPIE*, vol. 8473, 2012, Art. no. 847309, doi: 10.1117/12.929576.

[10] E. Krassowski, S. Großer, M. Turek, A. Henning, and H. Zhao, "Investigation of monocrystalline p-type PERC cells featuring the laser enhanced contact optimization process and new LECO paste," *AIP Conf. Proc.*, vol. 2367, 2021, Art. no. 020005, doi: 10.1063/5.0056380.

[11] R. M. Langford and C. Clinton, "In situ lift-out using a FIB-SEM system," *Micron*, vol. 35, pp. 607–611, 2004, doi: 10.1016/j.micron.2004.03.002.

[12] C. Ballif, D. M. Huljic, G. Willeke, and A. Hessler-Wyser, "Silver thick-film contacts on highly doped n-type silicon emitters: Structural and electronic properties of the interface," *Appl. Phys. Lett.*, vol. 82, no. 12, pp. 1878–1880, 2003, doi: 10.1063/1.1562338.

[13] A. Mette, "New concepts for front side metallization of industrial silicon solar cells," Ph.D. dissertation, Fraunhofer Inst. Solar Energy Systems, Freiburg im Breisgau, Germany, 2007.

[14] E. Cabrera, S. Olibet, J. Glatz-Reichenbach, R. Kopecek, D. Reinke, and G. Schubert, "Experimental evidence of direct contact formation for the current transport in silver thick film metallized silicon emitters," *J. Appl. Phys.*, vol. 110, 2011, Art. no. 114511, doi: 10.1063/1.3665718.

[15] R. Hoenig *et al.*, "The nature of screen printed front side silver contacts - Results of the project Mikrosol," *Energy Procedia*, vol. 43, pp. 27–36, 2013, doi: 10.1016/j.egypro.2013.11.085.

[16] F. M. d'Heurle, "Interfaces in silicon technology," *J. Electron. Mater.*, vol. 27, pp. 1138–1147, 1998.

[17] A. Tilke, L. Pescini, H. Lorenz, and R. H. Blick, "Electron-phonon interaction in suspended highly doped silicon nanowires," *Nanotechnology*, vol. 13, pp. 491–494, 2002, doi: 10.1088/0957-4484/13/4/310.

[18] R. W. Olesinski, A. B. Gokhale, and G. J. Abbaschian, "The Ag-Si (Silver-Silicon) system," *Bull. Alloy Phase Diagrams*, vol. 10, pp. 635–640, 1989, doi: 10.1007/BF02877631.

[19] C. Kim *et al.*, "Effects of current-injection firing with Ag paste in a boron emitter," *Sci. Rep.*, vol. 6, 2016, Art. no. 21553, doi: 10.1038/srep21553.